

HAD: Hybrid Architecture Distillation Outperforms Teacher in Genomic Sequence Modeling

Hexiong Yang^{1,3} Mingrui Chen^{2,3,4}

Huaibo Huang^{2,3} Junxian Duan^{2,3} Jie Cao^{2,3} Zhen Zhou⁵ Ran He^{2,3}

¹School of Advanced Interdisciplinary Science, University of Chinese Academy of Sciences

²School of Artificial Intelligence, University of Chinese Academy of Sciences

³NLPR&MAIS, Institute of Automation, Chinese Academy of Sciences

⁴Zhongguancun Academy ⁵Nanjing University

yanghexiong2002@gmail.com, charmier2003@gmail.com, rhe@nlpr.ia.ac.cn

Abstract

Inspired by the great success of Masked Language Modeling (MLM) in the natural language domain, the paradigm of self-supervised pre-training and fine-tuning has also achieved remarkable progress in the field of DNA sequence modeling. However, previous methods often relied on massive pre-training data or large-scale base models with huge parameters, imposing a significant computational burden. To address this, many works attempted to use more compact models to achieve similar outcomes but still fell short by a considerable margin. In this work, we propose a Hybrid Architecture Distillation (HAD) approach, leveraging both distillation and reconstruction tasks for more efficient and effective pre-training. Specifically, we employ the NTv2-500M as the teacher model and devise a grouping masking strategy to align the feature embeddings of visible tokens while concurrently reconstructing the invisible tokens during MLM pre-training. To validate the effectiveness of our proposed method, we conducted comprehensive experiments on the Nucleotide Transformer Benchmark and Genomic Benchmark. Compared to models with similar parameters, our model achieved excellent performance. **More surprisingly**, it even surpassed the *distillation ceiling*-teacher model on some sub-tasks, which is more than $500 \times$ larger. Lastly, we utilize t-SNE for more intuitive visualization, which shows that our model can gain a sophisticated understanding of the intrinsic representation pattern in genomic sequences.

1 Introduction

In the realm of DNA sequence modeling, the paradigm of self-supervised pre-training followed by fine-tuning is catalyzing significant advancements, fundamentally reshaping how genomic data is interpreted and utilized [1, 2]. Within this transformative landscape, masked language modeling (MLM) has prominently emerged as a primary technique. By pre-training models on vast, unlabeled DNA datasets, these methods can learn effective representations for downstream genomic tasks [3, 4, 5, 6, 7, 8]. These learned representations are foundational for numerous downstream genomic tasks, greatly improving predictive capabilities and fostering deeper biological insights [9, 8].

Scaling up the parameter size of models, especially in Transformers-based work [3, 4, 5], is a prevalent method for enhancing pre-trained models. Though this approach can often bring certain performance gain, it inevitably results in considerably higher computational demands [10].

Consequently, an alternative and also crucial research direction that focuses on novel, compact and efficient architectures has emerged [6, 7, 11]. However, although these compact architectures provide

desirable computational efficiency, they often struggle to match the in-depth representation learning and performance of those larger or more extensively pre-trained counterparts [5, 7].

Compact models, despite their efficient pre-training capable of processing tens of billions of nucleotide tokens [7], often hit capacity limits early, restricting their ability to learning complex patterns from massive genomic data. Conversely, larger models undergo far more extensive training [5] for deeper extraction of subtle biological feature. Thus, achieving profound representation learning in compact models remains a key challenge.

To overcome these limitations, we propose a novel framework for genomic sequence modeling with Hybrid Architecture Distillation (HAD). HAD uses a hybrid student architecture to capture a wide range of DNA sequence features, from key local feature to the global interactions, within only 1M parameter. Based on a bidirectional Gated Delta Net (GDN) [12], it combines linear complexity with adaptive memory control via two complementary mechanisms: the gating mechanism selectively erases irrelevant or redundant non-functional sequence segments, the delta update rule accurately modifies memory by identifying specific short sequences. To integrate comprehensive global information, this GDN backbone is augmented with a self-attention layer [13, 14]. This hybrid approach harnesses combined strengths, effectively integrating GDN’s proficiency in capturing local and long-range sequential patterns with attention’s capacity for unifying global context.

Our model empowers compact architecture with deep biological understanding through hybrid learning tasks, implemented within an innovative parallel dual-branch pretraining framework. These tasks distinctively combine two complementary objectives: a high-level feature alignment with a large teacher model using *visible* DNA nucleotides, and a low-level nucleotide reconstruction task focusing on *masked* positions. For the high-level alignment, our devised grouping masking strategy directs the student to align its feature embeddings of visible tokens with those from the teacher model, Nucleotide Transformer v2 [5](>500M), to gain more sophisticated biological insights. Concurrently, the low-level reconstruction branch try to predict the original identities of masked nucleotides by using the learned representation of visible nucleotides from aliment branch as context, which is implemented by a cross-attention mechanism and motivates our model to learn fundamental DNA sequence patterns and local grammar. This hybrid framework ensures HAD develops both profound representation and fine-grained understanding of DNA sequence.

To validate our proposed method’s effectiveness, we conduct comprehensive evaluation on the widely used Nucleotide Transformer Benchmark and Genomic Benchmark. Our compact model with only 1M-parameter exhibited notable efficacy, not only outperforming competing models of similar parameter size but also *surprisingly* outperforms its teacher model with 500M-parameter. Furthermore, we perform more intuitive visual analysis based on t-SNE, which further reveals that our model can learn intrinsic feature pattern and discriminative genomic representation from diverse DNA categories. These observations confirm our approach’s effectiveness for genomic sequence modeling and various downstream tasks.

2 Related Work

2.1 Network Architecture For DNA Modeling

In recent years, research in DNA sequence modeling has increasingly focused on the development of more efficient model architectures, particularly in the context of Transformer-based models. Notable works such as DNABERT [3], DNABERT2 [4], and Nucleotide Transformer [5] have successfully employed standard Transformers as their backbone networks, achieving impressive performance in genomic sequence tasks. However, these models are not without limitations, especially their scalability to long-sequence modeling and their relatively high inference costs. To address these challenges, recent advancements have turned to more efficient modeling approaches[15, 16, 17, 18, 19, 20, 21, 22, 12, 23, 24]. For instance, HyenaDNA [6] introduces the Hyena operator, which reduces the model size to approximately 6.6M parameters while extending the model’s capacity to handle sequences up to 1M in length. Similarly, Caduceus [7] proposes a bidirectional and RC-equivariant Mamba block as the backbone, successfully incorporating the concept of selective structured state space models (SSMs)[20, 21] into the domain of DNA sequence modeling. In the realm of RNN-based models, recent studies have enhanced the global modeling capacity by incorporating a limited number of attention layers into the architecture. Additionally, recent works have introduced novel computational strategies, such as the Delta Rule [22, 12] and the Titans [23], which aim to improve

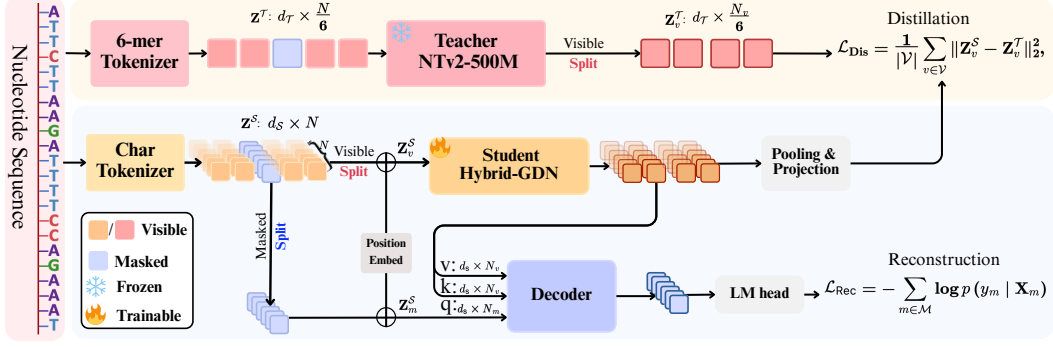


Figure 1: Proposed **Hybrid Architecture Distillation (HAD)** pre-training pipeline. The upper branch performs feature alignment on visible nucleotides, distilling *high-level* knowledge from a pre-trained teacher model to the student model. The lower branch focuses on the *low-level* reconstruction of masked nucleotides, leveraging contextual information from the student’s visible nucleotide representations.

memory management and retrieval performance for sequence modeling tasks[25, 26, 27, 28]. These developments indicate that adopting more efficient architectural designs and advanced computational strategies can overcome the inherent limitations of existing models, offering promising avenues for progress in DNA sequence modeling. This paper explores the potential of hybrid architectures as backbone networks for DNA modeling, aiming to advance the field through these innovative approaches.

2.2 Knowledge Distillation For DNA Modeling

Knowledge distillation (KD) [29, 30, 31] is a model compression technique that transfers knowledge from a large, high-capacity teacher model to a lightweight student model, enabling the latter to mimic the teacher’s behavior while reducing computational costs. Initially proposed by [32], KD leverages soft targets derived from the teacher’s output distribution rather than relying solely on ground-truth labels, thereby capturing richer inter-class relationships and enhancing generalization. Over time, KD has evolved into diverse paradigms, including feature-based distillation (*e.g.*, aligning intermediate representations), contrastive distillation (*e.g.*, preserving sample similarity structures), and relational distillation (*e.g.*, modeling geometric relationships). Recent advancements extend KD to cross-architecture settings, enabling knowledge transfer between heterogeneous model families (*e.g.*, Transformer→MLP), and self-distillation frameworks where the student iteratively refines its own outputs. In masked image modeling (MIM)[33, 34, 35, 36, 37, 38], where models learn by reconstructing masked regions of images, distillation has been instrumental in compressing large vision transformers (ViTs). For instance, feature-based distillation aligns intermediate attention maps between teacher and student models, preserving spatial-semantic patterns critical for reconstruction. While KD in DNA pretraining remains underexplored, insights from related domains suggest promising directions, such as Distilled DeepConsensus [39] and FinDNA [40], which applied KD and self-distillation techniques in the DNA correction and prediction tasks respectively. Analogously, DNA pretraining could leverage feature distillation to align latent representations of genomic sequences between teacher and student models, preserving motifs and regulatory patterns. In this paper, we will dive into this question and explore the potential of the knowledge distillation for hybrid architectures.

3 Methodology

3.1 Overall Pipeline

Traditional self-supervised learning for DNA sequences, such as Masked Language Modeling (MLM), typically processes a partially masked input sequence \mathbf{X}_m (derived from \mathbf{X}) through a unified encoder to predict the original nucleotides at masked positions m , optimized via a reconstruction objective:

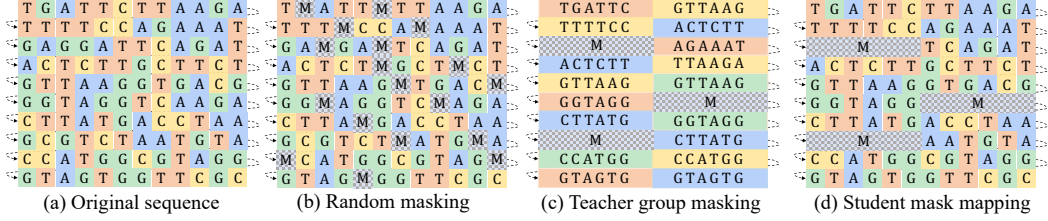


Figure 2: Two-stage masking strategy in HAD. This strategy is designed to prevent information leakage and enhance feature learning for the student model during distillation.

$$\mathcal{L}_{\text{Rec}} = - \sum_{m \in \mathcal{M}} \log p(y_m | \mathbf{X}_m), \quad (1)$$

where \mathcal{M} is the set of masked positions and $p(y_m | \mathbf{X}_m)$ represents the predicted probability of y_i given $\mathbf{X}_{\mathcal{M}}$. However, conventional MLM may not fully enable compact models to learn the deep features seen in much larger, extensively pre-trained models, especially when leveraging massive datasets. Thus, our Hybrid Architecture Distillation (HAD) framework significantly innovates upon this to bridge this gap by introducing a dual-branch pipeline. This design enables synergistic learning through two distinct yet complementary objectives: high-level feature alignment on visible nucleotides and low-level reconstruction of masked nucleotides, moving beyond the single-stream processing of conventional MLM.

The overall pipeline of HAD is illustrated in Figure 1. It begins by conceptually dividing the input sequence \mathbf{X} into visible nucleotides \mathbf{X}_v and masked positions \mathbf{X}_m . In the first branch, the student model \mathcal{S} processes \mathbf{X}_v (via its character-level tokenizer) into a hidden representation \mathbf{Z}_v^S . This is then aligned with the corresponding visible representation \mathbf{Z}_v^T derived from a large, pre-trained teacher model \mathcal{T} (which processes the full \mathbf{X} using its k -mer tokenizer and backbone, followed by filtering for visible parts). This feature-level distillation provides explicit high-level guidance. The second branch reconstructs the nucleotides at masked positions. For this, a decoder module integrates contextual information from the student’s visible nucleotide representations \mathbf{Z}_v^S with initial embeddings derived from the masked positions $\mathbf{X}_{\mathcal{M}}$. This integration yields context-aware representations for the masked nucleotides, $\mathbf{Z}_{\mathcal{M}}^S$. An LM Head subsequently maps these representations $\mathbf{Z}_{\mathcal{M}}^S$ to vocabulary logits to predict their original types, optimized with a loss analogous to \mathcal{L}_{Rec} . Thus, HAD distinctively conditions masked nucleotide reconstruction on information from the visible pathway, a key departure from standard MLM’s reliance on local masked context alone.

3.2 Hybrid Learning Tasks

Masking Strategy for Tokenizer Mismatch. Traditional random nucleotide masking is unsuitable for our hybrid learning task, as such strategies can create information inconsistencies and leakage during feature alignment between the k -mer level teacher and character-level student models, impairing distillation. To ensure consistent information and effective feature alignment, we therefore propose a two-stage mask sampling method.

Specifically, the first stage implements “teacher group masking” at the k -mer level (Figure 2c). Here, we randomly select 15% of k -mer units (*e.g.*, for a sequence of length N and 6-mers, $N/6$ units) to define the masked regions for the teacher model. By masking entire k -mer blocks, it presents a more structurally coherent and challenging masked context. For our student model, which operates at a character-level, this encourages learning from larger obscured spans during distillation, thereby fostering the acquisition of more valuable, high-level features. The second stage then involves mapping these k -mer level mask indices to the corresponding character-level positions for the student model (Figure 2d). This two-stage approach ensures consistent mask positioning between the teacher and student, prevents information leakage, and importantly, enhances the quality of feature learning for the student through more meaningful group-level masking.

Feature Alignment of Visible Nucleotides. With the visible and masked nucleotide positions established by our two-stage masking strategy, the first of our hybrid learning tasks focuses on feature

alignment using these visible nucleotides. These visible segments are processed through the student model’s hybrid architecture (detailed in Section 3.3) to obtain its representation \mathbf{Z}_v^S . This student representation is then aligned with the corresponding features \mathbf{Z}_v^T derived from a large-scale teacher model, NTV2 (a pure Transformer architecture with 500M parameters). Pre-trained on a multi-species dataset using over 1 trillion tokens, the NTV2 teacher model exhibits strong biological representation capabilities. The primary goal of this alignment is to enable the student model to inherit the teacher’s sophisticated biological expertise and learned high-level features from the visible portions of the sequence.

The alignment process faces two main challenges: differing hidden dimensions and sequence length. The student model has a hidden dimension of $d_S = 128$, while the teacher model has $d_T = 1024$. Additionally, the student model uses a character-level tokenizer, producing sequences of length $L = N$, whereas the teacher model uses a k-mer tokenizer with $k = 6$, resulting in sequences of length $L_{k\text{-mer}} = \frac{N}{6}$. To address these, we first apply average pooling to the student model’s sequence representations, reducing the sequence length from L to $L_{k\text{-mer}}$ to match the teacher model’s output. This is done over non-overlapping 6-mer windows. After aligning the sequence length, we use a projection layer to map the student model’s hidden representations from d_S to d_T . These two operations align both the sequence length and feature dimensions, facilitating appropriate feature alignment.

The feature alignment is achieved by minimizing the Mean Squared Error (MSE) loss between the student and teacher model representations. Since only visible nucleotides are aligned, the teacher model extracts representations for visible nucleotides based on pre-sampled mask indices. The MSE loss is computed as:

$$\mathcal{L}_{\text{Dis}} = \frac{1}{|\mathcal{V}|} \sum_{v \in \mathcal{V}} \|\mathbf{Z}_v^S - \mathbf{Z}_v^T\|_2^2, \quad (2)$$

where \mathcal{V} denotes the set of visible nucleotide positions. Within the sum, \mathbf{Z}_v^S is the student model’s representation at a visible position $v \in \mathcal{V}$, and \mathbf{Z}_v^T is the teacher model’s representation at the same position v . By minimizing this loss, we ensure that the student model effectively aligns its visible nucleotide representations with the teacher model’s.

Reconstruction of Masked Nucleotides. To preserve the model’s capability for low-level nucleotide understanding, a masked nucleotide reconstruction task remains essential. However, due to our framework’s clear division of visible and masked nucleotide processing pathways, a dedicated decoder mechanism is necessary for this reconstruction. In our approach for this task, the masked nucleotide positions are initialized randomly rather than using a fixed [MASK] token. We also ensure that positional information is added to the representations of both visible and masked nucleotides before they enter their respective model pathways. This explicit positional encoding preserves crucial spatial information, enabling accurate reconstruction of the original masked nucleotide positions.

For the Decoder, we use Cross Attention(CA), where the masked nucleotides act as the query, and the visible nucleotides serve as both the key and value. The masked nucleotides’ representations, as queries, attend to the visible nucleotides’ representations to produce the corresponding masked sequence. The CA operation is computed as follows:

$$\text{CA}(\mathbf{Q}_m, \mathbf{K}_v, \mathbf{V}_v) = \text{softmax}\left(\frac{\mathbf{Q}_m \mathbf{K}_v^T}{\sqrt{d_k}}\right) \mathbf{V}_v, \quad (3)$$

where \mathbf{Q}_m is the query (masked nucleotides), \mathbf{K}_v and \mathbf{V}_v are the key and value (visible nucleotides), and d_k is the dimensionality of the keys. This attention mechanism allows the model to focus on the relevant information in the visible nucleotides while reconstructing the masked nucleotides.

Finally, an LM Head maps the resulting masked representations \mathbf{Z}_m^S to vocabulary logits, producing a probability distribution for each masked nucleotide. The optimization objective for this reconstruction is to minimize a cross-entropy function analogous to \mathcal{L}_{Rec} (Same as Equation (1)).

3.3 Hybrid Student Architecture

Our hybrid architecture for DNA sequence modeling is founded on the Gated Delta Net (GDN) [22, 12]. The state \mathbf{S}_t of GDN at each time step t is dynamically updated based on its previous state

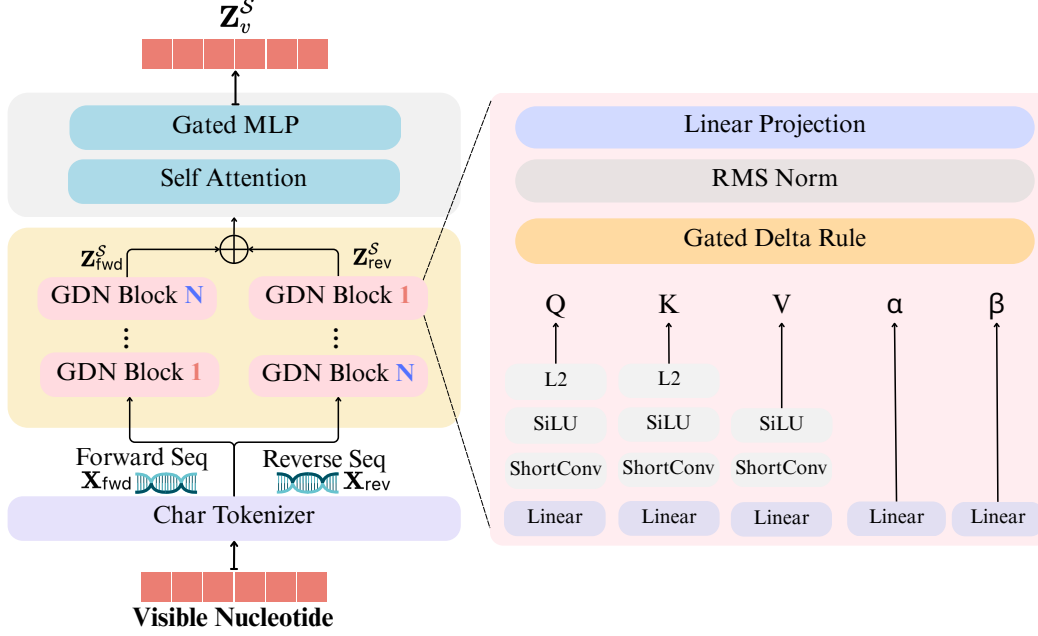


Figure 3: Hybrid architecture of our student model, combining a bidirectional Gated Delta Net (GDN) backbone with a self-attention layer for efficient sequential processing and global context integration within a compact 1.1M parameter budget. Within the GDN, α serves as a data-dependent gate controlling memory erasure, while β acts as the update strength from the delta rule.

\mathbf{S}_{t-1} and current inputs, following the principle:

$$\mathbf{S}_t = \mathbf{S}_{t-1} \left(\alpha_t \left(\mathbf{I} - \beta_t \mathbf{k}_t \mathbf{k}_t^T \right) \right) + \beta_t \mathbf{v}_t \mathbf{k}_t^T. \quad (4)$$

Equation (4) details how GDN dynamically updates its memory \mathbf{S}_t for our DNA sequence modeling, using complementary “Gated” and “Delta Rule” mechanisms. The gating, via α_t and the $(\mathbf{I} - \beta_t \mathbf{k}_t \mathbf{k}_t^T)$ term, allows the model to selectively clear or retain prior nucleotide context, effectively filtering information from less relevant DNA segments based on the current key \mathbf{k}_t . The Delta Rule component, $\beta_t \mathbf{v}_t \mathbf{k}_t^T$, then precisely incorporates features from the current input nucleotides (key \mathbf{k}_t , value \mathbf{v}_t), ensuring significant DNA patterns update the memory. To enable bidirectional modeling, we process the original sequence \mathbf{X}_{fwd} and its reverse \mathbf{X}_{rev} with separate GDN modules, yielding forward $\mathbf{Z}_{\text{fwd}}^S$ and reverse $\mathbf{Z}_{\text{rev}}^S$ hidden states. These are combined by reversing $\mathbf{Z}_{\text{rev}}^S$ and adding it to $\mathbf{Z}_{\text{fwd}}^S$, allowing the model to capture dependencies from both upstream and downstream contexts. To achieve efficient GPU utilization, GDN is parallelized using a chunk-wise method.

To further integrate global sequence information, the bidirectional GDN backbone is enhanced with an attention mechanism[41]. Specifically, following the final bidirectional GDN module, we append a single self-attention layer, implemented using Flash Attention [13, 14]. The output from this attention layer is then processed by a simple Gated MLP. This completes our hybrid architecture, designed to balance efficient sequential modeling with global contextual understanding.

4 Experiments

In this section, we present the experimental setup and results for evaluating our proposed method. Our model is evaluated against state-of-the-art baselines on the Nucleotide Transformer and Genomic Benchmarks[42]. We also use t-SNE for visualization, aiming to validate the feature learning capability transferred from the teacher to the student model within the HAD framework.

Table 1: **Nucleotide Transformer Benchmark Results.** Performance of HAD against baseline models and its NTv2 teacher. Results are means from 10-fold cross-validation with 10 random seeds; best performance is in **bold**, second-best is underlined. Error bars represent the range (maximum-minimum) across the 10 seeds. The final column, $\Delta_{\text{Student-Teacher}}$, shows the performance difference between HAD and its teacher.

Dataset Param.	Enformer[43] 252M	DNABERT-2[4] 117M	HyenaDNA[6] 1.6M	Caduceus[7] 1.9M	NT(Teacher)[5] 498.3M	HAD(Student) 1.1M	$\Delta_{\text{Student-Teacher}}$ -497.2M
<i>Histone Markers</i>							
H3	0.719 \pm 0.048	0.785 \pm 0.033	0.779 \pm 0.037	<u>0.815</u> \pm 0.048	0.784 \pm 0.047	0.822 \pm 0.007	+3.8%
H3K14ac	0.288 \pm 0.077	0.591 \pm 0.028	0.612 \pm 0.065	<u>0.631</u> \pm 0.026	0.551 \pm 0.021	0.684 \pm 0.041	+13.6%
H3K36me3	0.344 \pm 0.055	0.591 \pm 0.020	0.613 \pm 0.041	0.601 \pm 0.129	<u>0.625</u> \pm 0.013	0.653 \pm 0.031	+2.8%
H3K4me1	0.291 \pm 0.061	0.511 \pm 0.028	0.512 \pm 0.024	0.523 \pm 0.039	<u>0.550</u> \pm 0.021	0.571 \pm 0.037	+2.1%
H3K4me2	0.211 \pm 0.069	0.336 \pm 0.040	0.455 \pm 0.095	<u>0.487</u> \pm 0.170	0.319 \pm 0.045	0.562 \pm 0.033	+24.3%
H3K4me3	0.158 \pm 0.072	0.352 \pm 0.077	<u>0.549</u> \pm 0.056	0.544 \pm 0.045	0.410 \pm 0.033	0.643 \pm 0.052	+23.3%
H3K79me3	0.496 \pm 0.042	0.613 \pm 0.030	0.672 \pm 0.048	<u>0.697</u> \pm 0.077	0.626 \pm 0.026	0.712 \pm 0.022	+8.6%
H3K9ac	0.420 \pm 0.063	0.542 \pm 0.029	0.581 \pm 0.061	<u>0.622</u> \pm 0.030	0.562 \pm 0.040	0.656 \pm 0.023	+9.4%
H4	0.732 \pm 0.076	0.796 \pm 0.027	0.763 \pm 0.044	0.811 \pm 0.022	0.799 \pm 0.025	0.806 \pm 0.018	+0.7%
H4ac	0.273 \pm 0.063	0.463 \pm 0.041	0.564 \pm 0.038	<u>0.621</u> \pm 0.054	0.495 \pm 0.032	0.654 \pm 0.039	+15.9%
<i>Enhancer Annotation</i>							
Enhancer	0.451 \pm 0.108	0.516 \pm 0.098	0.517 \pm 0.117	0.546 \pm 0.073	0.548 \pm 0.144	0.571 \pm 0.075	+2.3%
Types	0.309 \pm 0.134	0.423 \pm 0.051	0.386 \pm 0.185	<u>0.439</u> \pm 0.054	0.424 \pm 0.132	0.467 \pm 0.073	+4.3%
<i>Promoter Annotation</i>							
All	0.954 \pm 0.006	<u>0.971</u> \pm 0.006	0.960 \pm 0.005	0.970 \pm 0.004	0.976 \pm 0.006	0.968 \pm 0.004	-0.8%
Non-TATA	0.955 \pm 0.010	<u>0.972</u> \pm 0.005	0.959 \pm 0.008	0.969 \pm 0.011	0.976 \pm 0.005	0.968 \pm 0.005	-0.8%
TATA	<u>0.960</u> \pm 0.023	0.955 \pm 0.021	0.944 \pm 0.040	0.953 \pm 0.016	0.966 \pm 0.013	0.958 \pm 0.009	-0.8%
<i>Splice Site Annotation</i>							
All	0.848 \pm 0.019	0.939 \pm 0.009	<u>0.956</u> \pm 0.011	0.940 \pm 0.027	0.983 \pm 0.008	0.911 \pm 0.016	-7.2%
Acceptor	0.914 \pm 0.028	<u>0.975</u> \pm 0.006	0.958 \pm 0.010	0.937 \pm 0.033	0.981 \pm 0.011	0.858 \pm 0.016	-12.3%
Donor	0.906 \pm 0.027	<u>0.963</u> \pm 0.006	0.949 \pm 0.024	0.948 \pm 0.025	0.985 \pm 0.022	0.887 \pm 0.045	-9.8%

4.1 Experiments Setting

Pre-training. We employed the hybrid architecture that incorporates both distillation and reconstruction tasks as described in Section 3. For comparison with baseline models, we used the exact same pre-training data[44] as in [6, 7], which adopts the training/validation split proposed by [43]. When pretraining on the human reference genome[44], we followed the RC equivariance inductive bias proposed by [7], implementing it using data augmentation, which has been proven to be an effective and straightforward approach. We chose a sequence length of 1026 for two key reasons: it’s suitable for our downstream tasks (most sequences in Nucleotide Transformer Benchmarks and Genomic benchmarks are $< 1k$ bp), and its divisibility by 6 (the teacher’s k -mer size) helps resolve tokenizer mismatches between our character-level student model and the k -mer based teacher model. Our student model itself is configured with 4 Gated Delta Net (GDN) blocks, each with a dimension of 128, resulting in a compact model with approximately 1.1 million parameters. Regarding the teacher model, NTv2-500M was selected as the source of high-level knowledge, providing rich feature representations.

Fine-tuning. We performed supervised training for each downstream task in both the Nucleotide Transformer benchmarks and the Genomic Benchmarks. Our fine-tuning protocol, including the use of post-hoc conjointing[45] for model RC invariance, strictly followed the configurations outlined in [7]. To ensure a fair comparison, all baselines and their reported results were adopted directly from [7], reflecting our identical experimental setup. Evaluation metrics were chosen per benchmark: for Nucleotide Transformer Benchmarks, following [6, 7], we used Matthews Correlation Coefficient (MCC) for histone marker tasks, F1 score for enhancer, promoter, and splice site annotation tasks (with accuracy for the “splice site all” task). All Genomic Benchmark tasks were evaluated using Top-1 accuracy.

4.2 Downstream Evaluation

Nucleotide Transformer Benchmarks. The evaluation of our proposed HAD model on the Nucleotide Transformer Benchmarks is presented in Table 1. With only 1.1M parameters, HAD is the most compact model among all baselines, yet it demonstrates exceptional performance. It achieves leading results in the majority of Histone Marker tasks and all Enhancer Annotation tasks, securing the top position in 11 out of 18 tasks overall. Notably, as highlighted in the $\Delta_{\text{Student-Teacher}}$ column, HAD consistently outperforms its significantly larger teacher model (NTv2, 500M parameters) across

Table 2: **Genomic Benchmarks Results.** Performance of HAD against baseline models. Results are means from 5-fold cross-validation with 5 random seeds. The best performance in each row is in **bold**, and the second-best is underlined. Error bars represent the range (maximum-minimum) across the random seeds. The final row shows the average performance across all eight tasks, demonstrating HAD’s strong overall results on this benchmark.

Dataset	CNN[42]	HyenaDNA[6]	Mamba[7]	Caduceus[7]	HAD
Mouse Enhancers	0.715 \pm 0.087	0.780 \pm 0.025	0.743 \pm 0.054	0.754 \pm 0.074	0.788 \pm 0.033
Coding vs Intergenic	0.892 \pm 0.008	0.904 \pm 0.005	0.904 \pm 0.004	0.915 \pm 0.003	<u>0.913</u> \pm 0.003
Human vs Worm	0.942 \pm 0.002	0.964 \pm 0.002	0.967 \pm 0.002	0.973 \pm 0.001	<u>0.971</u> \pm 0.001
Human Enhancer Cohn	0.702 \pm 0.021	0.729 \pm 0.014	0.732 \pm 0.029	0.747 \pm 0.004	<u>0.744</u> \pm 0.010
Human Enhancer Ensembl	0.744 \pm 0.122	0.849 \pm 0.006	0.862 \pm 0.008	<u>0.893</u> \pm 0.008	0.909 \pm 0.004
Human Regulatory	0.872 \pm 0.005	0.869 \pm 0.012	0.814 \pm 0.211	<u>0.872</u> \pm 0.011	0.882 \pm 0.012
Human OCR Ensembl	0.698 \pm 0.013	0.783 \pm 0.007	0.815 \pm 0.002	<u>0.828</u> \pm 0.006	0.832 \pm 0.003
Human NonTATA Promoters	0.861 \pm 0.009	0.944 \pm 0.002	0.933 \pm 0.007	<u>0.946</u> \pm 0.007	0.960 \pm 0.008
Average	0.803	0.853	0.846	<u>0.866</u>	0.875

numerous tasks, despite utilizing approximately 497.2M fewer parameters. This outcome underscores that the feature alignment process integral to HAD not only facilitates effective knowledge transfer but also empowers the student model to surpass the teacher’s performance ceiling, thereby significantly enhancing its learning and capabilities on downstream genomic tasks.

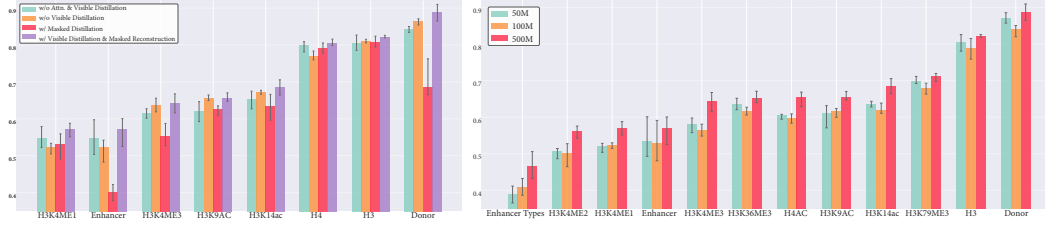


Figure 4: Ablation on pretraining scheme with different model architectures (left) and teacher model size (right)

Genomic Benchmarks. We further evaluated HAD on the Genomic Benchmarks, with results detailed in Table 2. The selection of baseline models for comparison remained consistent with those in [7]. In five of the eight downstream tasks within these benchmarks, our HAD model achieved the highest score among the evaluated baselines. Encouragingly, HAD’s average performance score of **0.875** across all tasks in these benchmarks was the highest among all reported baselines.

4.3 Ablation Study

Ablation of Different Architectures. To investigate the effectiveness of our overall HAD framework, we conducted an ablation study on the Nucleotide Transformer benchmarks (Figure 4 left). Our full model (“HAD w/ Visible Distillation & Masked Reconstruction”), with its hybrid architecture and dual-branch pretraining (visible distillation and masked reconstruction), was compared against variants lacking key components or using altered training strategies. These included removing self-attention and visible distillation (“HAD w/o Attn. & Visible Distillation”; GDN backbone, MLM-only), omitting only visible distillation (“HAD w/o Visible Distillation”; hybrid architecture, MLM-only), and distilling only from masked positions (“HAD w/ Masked Distillation”). The full HAD model significantly outperformed these ablations, highlighting that its hybrid architecture and dual-branch learning strategy are crucial for its superior performance.

Table 3 further details the pre-training losses for these ablated architectures. Among the MLM-exclusive versions (“GDN w/o Attn.” and “GDN w/ Attn.”), both targeted masked nucleotide reconstruction; the attention-equipped version achieved lower Cross-Entropy (CE) reconstruction loss, indicating more effective pre-training. For distillation approaches, the MSE loss from “ \mathcal{M} Dis.” (masked distillation) was lower than the visible distillation MSE component of “ \mathcal{V} Dis. & \mathcal{M} Rec.”. This discrepancy with the latter model’s established superior downstream performance could be explained by two factors: first, visible distillation is more challenging due to a larger number of targets; and second, component pre-training losses often misalign with overall downstream task performance.

Table 3: Validation loss for different architectures.

Arch.	Step				
	2k	4k	6k	8k	10k
Masked Language Modeling					
GDN w/o Attn.	1.0422	1.0290	1.0202	1.0127	1.0090
GDN w/ Attn.	1.0489	1.0273	1.0154	1.0068	1.0033
Masked Language Modeling + Distillation					
\mathcal{M} Dis.	0.3167	0.3149	0.3111	0.2994	0.2901
\mathcal{V} Dis. & \mathcal{M} Rec.	0.3177	0.3164	0.3143	0.3118	0.3049

Table 4: Perplexity scores with different teacher models.

Teacher Model	Step				
	2k	4k	6k	8k	10k
Masked Language Modeling + Distillation					
50M	5.876	5.835	5.814	5.797	5.785
100M	5.720	5.679	5.646	5.622	5.609
500M	5.217	4.903	4.708	4.599	4.538

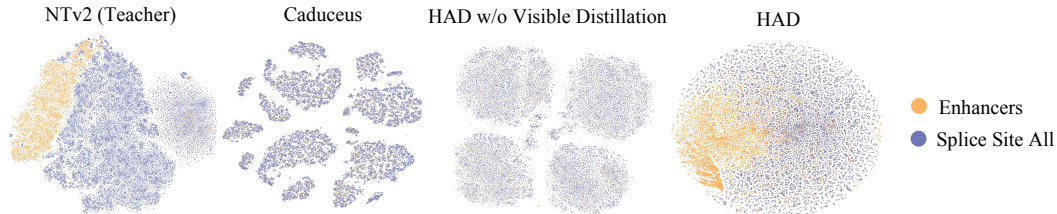


Figure 5: t-SNE visualization of pre-trained model representations on select downstream task data. The clustering visually demonstrates HAD’s effective knowledge transfer from its teacher NTv2 through the distillation branch, particularly for distinguishing Enhancer-related features.

Ablation of Different Teacher Models. We further investigated the impact of teacher model size on distillation performance by ablating the teacher component, employing NTv2 variants with 50M, 100M, and 500M parameters. As illustrated in Figure 4 (right), a significant enhancement in the student model’s downstream task performance was contingent upon guidance from the 500M parameter teacher. This observation highlights that a teacher model must possess substantial representational capacity, likely a product of comprehensive pretraining on extensive nucleotide data, to serve as an effective source of rich features for successful distillation to a smaller student architecture.

Further supporting this, the pre-training perplexity scores of these teacher models (Table 4) show a clear hierarchy: the 500M teacher achieved the lowest perplexity, followed by the 100M and 50M models across all evaluated training steps. This superior intrinsic language modeling capability of the largest teacher model likely underpins its effectiveness as a richer feature source for distillation.

4.4 Qualitative Analysis

To investigate the effectiveness of feature learning specifically imparted by the distillation process within our HAD framework, we employed t-SNE [46] to visualize representations from several models. We compared our full HAD model against the teacher model (NTv2-500M [5]), Caduceus [7], and the ablation variant “HAD w/o Visible Distillation” described in Section 4.3. These models were used as feature extractors for downstream task data from *Enhancers* and *splice site all*. As visualized in Figure 5, the NTv2-500M teacher model exhibits a strong capability to distinguish *Enhancers*. In contrast, both Caduceus and the “HAD w/o Visible Distillation” ablation fail to form meaningful clusters for these enhancer features. Conversely, our complete HAD model clearly learns and separates these enhancer-related features, effectively mirroring its teacher’s discriminative ability. This t-SNE analysis underscores that HAD successfully acquires high-level feature representations from the teacher model through the proposed distillation mechanism.

5 Conclusion

We have introduced HAD, an effective framework for DNA sequence modeling that utilize hybrid learning tasks, integrating feature alignment with masked nucleotide reconstruction. Our compact (1.1M parameter) student model thereby learns rich, high-level biological features by distilling knowledge from an extensively pre-trained and significantly larger teacher. Across different downstream tasks, HAD not only outperformed most models with comparable parameters but also surprisingly exceeded the performance of its $500\times$ larger teacher model. Finally, interpretable t-SNE analysis visually showcased HAD’s effective knowledge transfer through its robust learning of discriminative features.

References

- [1] Kathleen M Chen, Aaron K Wong, Olga G Troyanskaya, and Jian Zhou. A sequence-based global map of regulatory activity for deciphering human genetics. *Nature genetics*, 54(7):940–949, 2022.
- [2] Pengcheng Zhang, Lei Wei, Jiaqi Li, and Xiaowo Wang. Artificial intelligence-guided strategies for next-generation biological sequence design. *National Science Review*, 11(11):nwae343, 2024.
- [3] Yanrong Ji, Zhihan Zhou, Han Liu, and Ramana V Davuluri. Dnabert: pre-trained bidirectional encoder representations from transformers model for dna-language in genome. *Bioinformatics*, 37(15):2112–2120, 2021.
- [4] Zhihan Zhou, Yanrong Ji, Weijian Li, Pratik Dutta, Ramana Davuluri, and Han Liu. Dnabert-2: Efficient foundation model and benchmark for multi-species genome. *arXiv preprint arXiv:2306.15006*, 2023.
- [5] Hugo Dalla-Torre, Liam Gonzalez, Javier Mendoza-Revilla, Nicolas Lopez Carranza, Adam Henryk Grzywaczewski, Francesco Oteri, Christian Dallago, Evan Trop, Bernardo P de Almeida, Hassan Sirelkhatim, et al. Nucleotide transformer: building and evaluating robust foundation models for human genomics. *Nature Methods*, pages 1–11, 2024.
- [6] Eric Nguyen, Michael Poli, Marjan Faizi, Armin Thomas, Michael Wornow, Callum Birch-Sykes, Stefano Massaroli, Aman Patel, Clayton Rabideau, Yoshua Bengio, et al. Hyenadna: Long-range genomic sequence modeling at single nucleotide resolution. *Advances in neural information processing systems*, 36:43177–43201, 2023.
- [7] Yair Schiff, Chia-Hsiang Kao, Aaron Gokaslan, Tri Dao, Albert Gu, and Volodymyr Kuleshov. Caduceus: Bi-directional equivariant long-range dna sequence modeling. *arXiv preprint arXiv:2403.03234*, 2024.
- [8] Siyuan Li, Zedong Wang, Zicheng Liu, Di Wu, Cheng Tan, Jiangbin Zheng, Yufei Huang, and Stan Z. Li. VQDNA: unleashing the power of vector quantization for multi-species genomic sequence modeling. In *Forty-first International Conference on Machine Learning, ICML 2024, Vienna, Austria, July 21-27, 2024*. OpenReview.net, 2024.
- [9] Johannes Linder, Divyanshi Srivastava, Han Yuan, Vikram Agarwal, and David R Kelley. Predicting rna-seq coverage from dna sequence as a unifying model of gene regulation. *Nature Genetics*, pages 1–13, 2025.
- [10] Jinghan Ru, Yuxin Xie, Xianwei Zhuang, Yuguo Yin, and Yuexian Zou. Do we really have to filter out random noise in pre-training data for language models? *arXiv preprint arXiv:2502.06604*, 2025.
- [11] Micaela Elisa Consens, Ben Li, Anna R Poetsch, and Stephen Gilbert. Genomic language models could transform medicine but not yet. *npj Digital Medicine*, 8(1):212, 2025.
- [12] Songlin Yang, Jan Kautz, and Ali Hatamizadeh. Gated delta networks: Improving mamba2 with delta rule. *arXiv preprint arXiv:2412.06464*, 2024.
- [13] Tri Dao, Daniel Y. Fu, Stefano Ermon, Atri Rudra, and Christopher Ré. FlashAttention: Fast and memory-efficient exact attention with IO-awareness. In *Advances in Neural Information Processing Systems (NeurIPS)*, 2022.
- [14] Tri Dao. FlashAttention-2: Faster attention with better parallelism and work partitioning. In *International Conference on Learning Representations (ICLR)*, 2024.
- [15] Qihang Fan, Huaibo Huang, and Ran He. Breaking the low-rank dilemma of linear attention. *CoRR*, abs/2411.07635, 2024.
- [16] Qihang Fan, Huaibo Huang, Mingrui Chen, Hongmin Liu, and Ran He. RMT: retentive networks meet vision transformers. In *IEEE/CVF Conference on Computer Vision and Pattern Recognition, CVPR 2024, Seattle, WA, USA, June 16-22, 2024*, pages 5641–5651. IEEE, 2024.
- [17] Qihang Fan, Huaibo Huang, Jiyang Guan, and Ran He. Rethinking local perception in lightweight vision transformer. *CoRR*, abs/2303.17803, 2023.
- [18] Qihang Fan, Huaibo Huang, Mingrui Chen, and Ran He. Vision transformer with sparse scan prior. *arXiv preprint arXiv:2405.13335*, 2024.
- [19] Qihang Fan, Huaibo Huang, Mingrui Chen, and Ran He. Semantic equitable clustering: A simple, fast and effective strategy for vision transformer. *arXiv preprint arXiv:2405.13337*, 2024.

- [20] Albert Gu and Tri Dao. Mamba: Linear-time sequence modeling with selective state spaces. *arXiv preprint arXiv:2312.00752*, 2023.
- [21] Tri Dao and Albert Gu. Transformers are ssms: Generalized models and efficient algorithms through structured state space duality. *arXiv preprint arXiv:2405.21060*, 2024.
- [22] Songlin Yang, Bailin Wang, Yu Zhang, Yikang Shen, and Yoon Kim. Parallelizing linear transformers with the delta rule over sequence length. *arXiv preprint arXiv:2406.06484*, 2024.
- [23] Ali Behrouz, Peilin Zhong, and Vahab Mirrokni. Titans: Learning to memorize at test time. *arXiv preprint arXiv:2501.00663*, 2024.
- [24] Yutao Sun, Li Dong, Shaohan Huang, Shuming Ma, Yuqing Xia, Jilong Xue, Jianyong Wang, and Furu Wei. Retentive network: A successor to transformer for large language models. *arXiv preprint arXiv:2307.08621*, 2023.
- [25] Simran Arora, Sabri Eyuboglu, Aman Timalisina, Isys Johnson, Michael Poli, James Zou, Atri Rudra, and Christopher Ré. Zoology: Measuring and improving recall in efficient language models. *arXiv preprint arXiv:2312.04927*, 2023.
- [26] Kaiyue Wen, Xingyu Dang, and Kaifeng Lyu. Rnns are not transformers (yet): The key bottleneck on in-context retrieval. *arXiv preprint arXiv:2402.18510*, 2024.
- [27] Yuguo Yin, Yuxin Xie, Wenyuan Yang, Dongchao Yang, Jinghan Ru, Xianwei Zhuang, Liming Liang, and Yuexian Zou. Atri: Mitigating multilingual audio text retrieval inconsistencies by reducing data distribution errors. *arXiv preprint arXiv:2502.14627*, 2025.
- [28] Ekin Akyürek, Bailin Wang, Yoon Kim, and Jacob Andreas. In-context language learning: Architectures and algorithms. *arXiv preprint arXiv:2401.12973*, 2024.
- [29] Jianping Gou, Baosheng Yu, Stephen J Maybank, and Dacheng Tao. Knowledge distillation: A survey. *International Journal of Computer Vision*, 129(6):1789–1819, 2021.
- [30] Jiayi Tang, Rakesh Shivanna, Zhe Zhao, Dong Lin, Anima Singh, Ed H Chi, and Sagar Jain. Understanding and improving knowledge distillation. *arXiv preprint arXiv:2002.03532*, 2020.
- [31] Dan Busbridge, Amitis Shidani, Floris Weers, Jason Ramapuram, Etai Littwin, and Russ Webb. Distillation scaling laws. *arXiv preprint arXiv:2502.08606*, 2025.
- [32] Geoffrey Hinton, Oriol Vinyals, and Jeff Dean. Distilling the knowledge in a neural network. *arXiv preprint arXiv:1503.02531*, 2015.
- [33] Yue Cao, Zhenda Xie, Bin Liu, Yutong Lin, Zheng Zhang, and Han Hu. Parametric instance classification for unsupervised visual feature learning. *Advances in neural information processing systems*, 33:15614–15624, 2020.
- [34] Xiaoyi Dong, Jianmin Bao, Ting Zhang, Dongdong Chen, Weiming Zhang, Lu Yuan, Dong Chen, Fang Wen, and Nenghai Yu. Peco: Perceptual codebook for bert pre-training of vision transformers. In *AAAI*, 2023.
- [35] Zhenda Xie, Zheng Zhang, Yue Cao, Yutong Lin, Jianmin Bao, Zhuliang Yao, Qi Dai, and Han Hu. Simmim: A simple framework for masked image modeling. In *CVPR*, pages 9653–9663, 2022.
- [36] Sanghyun Woo, Shoubhik Debnath, Ronghang Hu, Xinlei Chen, Zhuang Liu, In So Kweon, and Saining Xie. Convnext v2: Co-designing and scaling convnets with masked autoencoders. In *Proceedings of the IEEE/CVF Conference on Computer Vision and Pattern Recognition*, pages 16133–16142, 2023.
- [37] Maxime Oquab, Timothée Darcet, Théo Moutakanni, Huy Vo, Marc Szafraniec, Vasil Khalidov, Pierre Fernandez, Daniel Haziza, Francisco Massa, Alaaeldin El-Nouby, et al. Dinov2: Learning robust visual features without supervision. *arXiv preprint arXiv:2304.07193*, 2023.
- [38] Jinghao Zhou, Chen Wei, Huiyu Wang, Wei Shen, Cihang Xie, Alan Yuille, and Tao Kong. Image bert pre-training with online tokenizer. In *ICLR*, 2022.
- [39] Anastasiya Belyaeva, Joel Shor, Daniel E Cook, Kishwar Shafin, Daniel Liu, Armin Töpfer, Aaron M Wenger, William J Rowell, Howard Yang, Alexey Kolesnikov, et al. Knowledge distillation for fast and accurate dna sequence correction. *arXiv preprint arXiv:2211.09862*, 2022.
- [40] Tong Yu, Lei Cheng, Ruslan Khalitov, Erland B Olsson, and Zhirong Yang. Self-distillation improves self-supervised learning for dna sequence inference. *Neural Networks*, 183:106978, 2025.

- [41] Ashish Vaswani, Noam Shazeer, Niki Parmar, Jakob Uszkoreit, Llion Jones, Aidan N Gomez, Łukasz Kaiser, and Illia Polosukhin. Attention is all you need. *Advances in neural information processing systems*, 30, 2017.
- [42] Katarína Grešová, Vlastimil Martinek, David Čechák, Petr Šimeček, and Panagiotis Alexiou. Genomic benchmarks: a collection of datasets for genomic sequence classification. *BMC Genomic Data*, 24(1):25, 2023.
- [43] Žiga Avsec, Vikram Agarwal, Daniel Visentin, Joseph R Ledsam, Agnieszka Grabska-Barwinska, Kyle R Taylor, Yannis Assael, John Jumper, Pushmeet Kohli, and David R Kelley. Effective gene expression prediction from sequence by integrating long-range interactions. *Nature methods*, 18(10):1196–1203, 2021.
- [44] Valerie A Schneider, Tina Graves-Lindsay, Kerstin Howe, Nathan Bouk, Hsiu-Chuan Chen, Paul A Kitts, Terence D Murphy, Kim D Pruitt, Françoise Thibaud-Nissen, Derek Albracht, et al. Evaluation of grch38 and de novo haploid genome assemblies demonstrates the enduring quality of the reference assembly. *Genome research*, 27(5):849–864, 2017.
- [45] Hannah Zhou, Avanti Shrikumar, and Anshul Kundaje. Towards a better understanding of reverse-complement equivariance for deep learning models in genomics. In *Machine Learning in Computational Biology*, pages 1–33. PMLR, 2022.
- [46] Laurens Van der Maaten and Geoffrey Hinton. Visualizing data using t-sne. *Journal of machine learning research*, 9(11), 2008.